

# Assessment of cervical lymph node metastases using indirect computed tomography lymphography with iopamidol in a tongue VX2 carcinoma model

Y SHU<sup>1</sup>, X XU<sup>2</sup>, Z WANG<sup>1</sup>, W DAI<sup>1</sup>, Y ZHANG<sup>1</sup>, Y YU<sup>3</sup>, Y SHA<sup>4</sup>, H WU<sup>1</sup>

Departments of <sup>1</sup>Otolaryngology-Head and Neck Surgery and <sup>4</sup>Radiology, Eye and ENT Hospital, Fudan University, <sup>2</sup>Department of Otolaryngology, Shanghai Seventh People's Hospital, and <sup>3</sup>Department of Biostatistics, School of Public Health, Fudan University, Shanghai, China

## Abstract

**Objective:** To investigate the performance of indirect computed tomography lymphography with iopamidol for detecting cervical lymph node metastases in a tongue VX2 carcinoma model.

**Materials and methods:** A metastatic cervical lymph node model was created by implanting VX2 carcinoma suspension into the tongue submucosa of 21 rabbits. Computed tomography images were obtained 1, 3, 5, 10, 15 and 20 minutes after iopamidol injection, on days 11, 14, 21 (six rabbits each) and 28 (three rabbits) after carcinoma transplantation. Computed tomography lymphography was performed, and lymph node filling defects and enhancement characteristics evaluated.

**Results:** Indirect computed tomography lymphography revealed bilateral enhancement of cervical lymph nodes in all animals, except for one animal imaged on day 28. There was significantly slower evacuation of contrast in metastatic than non-metastatic nodes. A total of 41 enhanced lymph nodes displayed an oval or round shape, or local filling defects. One lymph node with an oval shape was metastatic (one of 11, 9.1 per cent), while 21 nodes with filling defects were metastatic (21/30, 70 per cent). The sensitivity, specificity, accuracy, and positive and negative predictive values when using a filling defect diameter of 1.5 mm as a diagnostic criterion were 86.4, 78.9, 82.9, 82.6 and 83.3 per cent, respectively.

**Conclusion:** When using indirect computed tomography lymphography to detect metastatic lymph nodes, filling defects and slow evacuation of contrast agent are important diagnostic features.

**Key words:** Lymphography; Computed Tomography; Lymph Node; Neoplasm Metastasis; Head And Neck Neoplasms

## Introduction

In patients with malignancy, it is essential to establish the lymph node status, in order to guide therapeutic decisions and determine prognosis. At present, the diagnostic roles of the various available non-invasive lymphatic imaging modalities remain to be determined.<sup>1</sup>

Computed tomography (CT) and magnetic resonance imaging (MRI) are currently the most frequently used methods of assessing lymph node status. Their usefulness in this context depends heavily upon lymph node size and evidence of necrosis. However, some small metastatic lymph nodes may not contain central necrosis. In addition, CT and MRI have limited sensitivity for the detection of metastatic lymph nodes in the case of non-enlarged metastatic

nodes and small intranodal tumour deposits, and limited specificity in the case of enlarged inflammatory lymph nodes.<sup>2,3</sup>

The use of ultrasonography in lymph node assessment is limited by anatomical location. Even when ultrasonography is used together with fine needle aspiration, its sensitivity varies depending on operator experience and on whether sampling error has been introduced.

Positron emission tomography (PET) characterises the metabolic activity of the involved organ, but at the expense of anatomical definition.<sup>4</sup> The clinical potential of PET combined with CT is promising, but may be limited by a combination of limited sensitivity for small metastatic deposits and a relatively high number of false positive findings in the node-negative

neck.<sup>5</sup> In addition, the cost of PET is high and it is not readily available, especially in developing countries.<sup>6</sup>

Lymphography has the unique capability of demonstrating internal architectural derangement within normal-sized lymph nodes. However, conventional lymphography has in most contexts been replaced by cross-sectional imaging, especially CT, owing to its invasiveness, technical difficulties and potential side effects (including hypothyroidism, pulmonary embolism, local wound infection and hypersensitivity to ethiodised oil).<sup>7</sup>

Lymphography and CT are complementary techniques in the diagnosis and staging of malignancy.<sup>8</sup> In 1994, Worf *et al.* depicted successfully the intranodal distribution of macrophages within normal lymph nodes in rabbits and monkeys, using percutaneous CT lymphography with Perflubron®.<sup>9</sup> Using indirect CT lymphography with iodinated nanoparticles, Wisner *et al.* discovered architectural alterations in metastatic lymph nodes in pigs, including medullary filling defects.<sup>10</sup> Jiang *et al.* induced popliteal lymph node metastases by injecting VX2 cells into New Zealand White rabbits; 15 to 18 days later, percutaneous indirect CT lymphography using radiopaque nanoparticles showed homogeneous enhancement of normal node regions and no enhancement of cancer.<sup>11</sup> These results were in accordance with those obtained from histological analysis. However, Jiang *et al.* did not investigate quantitatively one important and reliable criterion for metastatic lymph node diagnosis on CT lymphography: filling defects.

In addition, maximum enhancement of regional lymph nodes has been observed 24 to 48 hours after injection of Perflubron or iodinated nanoparticles.<sup>9,10</sup>

Recently, indirect CT lymphography has been successfully employed to identify sentinel lymph nodes in the breast, oesophagus, lung, skin, and head and neck, using the non-ionic, iodinated, water-soluble contrast agent iopamidol.<sup>12–17</sup> To the best of our knowledge, iopamidol has not previously been used to differentiate metastatic from non-metastatic lymph nodes, or to analyse their characterisation on CT lymphography, either quantitatively or qualitatively.

In this study, a metastatic cervical lymph node model was established in rabbits. We evaluated the use of indirect CT lymphography with iopamidol to differentiate metastatic from non-metastatic cervical lymph nodes, using histopathological analysis as the reference standard.

## Materials and methods

### Tumour model

The study was approved by the animal care and use committee of Fudan University.

Twenty-one coeval, 12-month-old New Zealand White rabbits each weighing 2.5–3.0 kg served as the animal model. Tongue carcinoma and cervical lymph node metastasis were induced by injection of a VX2

cell mass suspension.<sup>18</sup> Each rabbit was anaesthetised with an intramuscular injection of 50 mg ketamine hydrochloride and 20 mg xylazine hydrochloride, 0.5 ml/kg body weight, while positioned supine on a specially designed operating table. The tongue was retracted and approximately 0.3 ml of VX2 carcinoma suspension was injected into the right ventrolateral submucosa, under sterile conditions.

### Indirect computed tomography lymphography

In order to investigate the resultant metastatic lymph nodes, indirect CT lymphography was performed on days 11 (in six animals), 14 (six animals), 21 (six animals) and 28 (three animals) after carcinoma implantation.

Animals were anaesthetised in the same manner as for tumour implantation, and imaged on a CT table in the supine position with the neck extended.

Transverse CT scanning was performed using a Siemens Somatom Sensation 10 scanner (Siemens, Forchheim, Bavaria, Germany) operated at 120 kV and 150 mAs with a 7–12 cm field of view and a 512 × 512 matrix.

Precontrast CT images were taken to eliminate the possibility of lymph node calcification. Approximately 0.5 ml of undiluted iopamidol (300 mg I/ml; Shanghai Bracco Sine Pharmaceutical, Shanghai, China) was injected gently into the ipsilateral peritumoural submucosa and contralateral normal ventrolateral submucosa of the tongue. The injections into each side of the tongue were performed within 1 minute of each other. Contiguous 1.5 mm thick CT images from the level of the tongue to the sternum were taken 1, 3, 5, 10, 15 and 20 minutes after iopamidol injection. Additional images were obtained at 5-minute intervals until lymphatic vessel or lymph node enhancement was no longer visible to the naked eye.

The enhanced lymph nodes were identified and their locations (corresponding to their position on CT lymphography) were marked on the skin with a painting pen.

### Image analysis

Computed tomography images were analysed using the Siemens Leonardo image workstation. The results were assessed by two radiologists blinded to each animal's lymph node status; disagreement was resolved by consensus.

When assessing lymph node enhancement, operator-defined 'regions of interest' were specified on consecutive CT images, for all opacified lymph nodes. Regions of interest encompassed as much of the lymph node as possible, and avoided the filling defect regions in irregularly shaped lymph nodes. The size and position of the region of interest remained unchanged on the image obtained at each time point, within the same lymph node and during the same examination.<sup>19</sup> The same lymph nodes were then identified on precontrast images, and the equivalent regions of interest defined on those images.

In addition, the shape and maximum axial diameter of all enhanced lymph nodes were recorded from the first postcontrast transverse CT lymphography images that showed peak enhancement of opacified lymph nodes, in order to avoid the potential 'wash-in' and 'wash-out' effects of contrast agents.<sup>16,20</sup>

In enhanced lymph nodes showing filling defects, we also calculated the filling defect diameter and intranodal filling defect ratio (i.e. the ratio between the area of filling defect and the area of lymph node).

Imaging results were then compared with histopathological findings.

### *Histopathological analysis*

After completing indirect CT lymphography, all rabbits were sacrificed with a lethal dose of intravenously administered sodium pentobarbital (90 mg/kg body weight).

A 1.5 cm long incision was made along the marked skin and the relevant lymph nodes were identified and resected carefully (referring to the detailed anatomical information derived from CT lymphography). If there was no enhancement on the postcontrast images, we removed target lymph nodes in sites matching the sites of enhancing lymph nodes in other animals (based on anatomical positions determined by CT lymphography, in optimally enhanced animals). We then performed complete dissection of the remaining cervical lymph nodes (including bilateral parotid lymph nodes and submandibular lymph nodes). The harvested lymph nodes, and their orientation, were labelled.

Tongue carcinomas were also removed.

The dissected lymph nodes and tongue carcinomas were fixed in 10 per cent formalin and embedded in paraffin. Specimens were sectioned in planes paralleling those of CT lymphography orientations, at 0.2 mm intervals along each lymph node, taking slices approximately 5 µm in width. Conventional sections of tongue carcinoma specimens were also obtained. All sections were stained with haematoxylin and eosin.

Histological sections were examined by two pathologists blinded to the imaging results. Discrepancies in interpretation were resolved by consensus.

### *Statistical analysis*

Statistical analysis was performed using Stata SE version 9.0 software.

In both metastatic and non-metastatic lymph nodes, CT attenuation values 1, 3, 5, 10, 15 and 20 minutes after contrast injection were treated as repeated measurements, with metastatic and non-metastatic lymph nodes as the two levels of the group factor and with measurement time as the repeated factor. A mixed model was then constructed for data analysis. The filling defect diameter and intranodal filling defect ratio were compared using the two-sample *t*-test and the Wilcoxon rank sum (Mann–Whitney)

test, respectively, for non-metastatic versus metastatic lymph nodes.

We evaluated the use of filling defect diameter and intranodal filling defect ratio as criteria for the differentiation of metastatic versus non-metastatic lymph nodes, and we calculated the sensitivities, specificities, accuracies, and positive and negative predictive values of these parameters for this diagnostic task. The diagnostic value of these two parameters was also compared using receiver operating characteristic curve analyses (i.e. calculating the area under the receiver operating characteristic curve). A probability level of  $p < 0.05$  was considered statistically significant.

## **Results and analysis**

### *Histopathology*

The presence of tongue carcinoma in all animals was confirmed by histopathological examination.

Forty-one enhanced lymph nodes were identified on CT lymphography. Guided by CT lymphography images, all 41 of these nodes were identified and resected from the expected location, i.e. lateral to the larynx and cricoid cartilage, below the sternothyroid muscle.

One additional lymph node, located in the same position, was harvested from one animal on day 28 after carcinoma implantation. This animal had shown an enhanced contralateral (left) lymph node but no enhanced ipsilateral (right) lymph node, on postcontrast CT lymphography.

Metastases to ipsilateral lymph nodes were verified histopathologically in four animals on day 11 after carcinoma implantation (four of six, 66.7 per cent), six animals on day 14 (six of six, 100 per cent), six animals on day 21 (six of six, 100 per cent) and three animals on day 28 (three of three, 100 per cent).

Metastases to bilateral lymph nodes were confirmed histopathologically in one animal on day 21 (one of six, 16.7 per cent) and three animals on day 28 (three of three, 100 per cent).

Overall, histopathological analysis indicated that 19 of the 42 dissected lymph nodes were non-metastatic (45.2 per cent) and 23 were metastatic (54.8 per cent). We therefore divided these dissected lymph nodes into two groups according to the presence or absence of metastasis on histopathological analysis.

The mean maximum axial diameter  $\pm$  standard deviation (SD) was  $7.49 \pm 1.81$  mm for metastatic lymph nodes and  $6.17 \pm 2.23$  mm for non-metastatic lymph nodes.

No metastases were found in the parotid or submandibular lymph nodes, in any of the 21 animals.

### *Computed lymphography*

Prior to administration of the contrast agent iopamidol, no noticeable lymph node calcification was visualised on CT, and lymphatic vessels and cervical lymph nodes could not be clearly identified (Figure 1a).

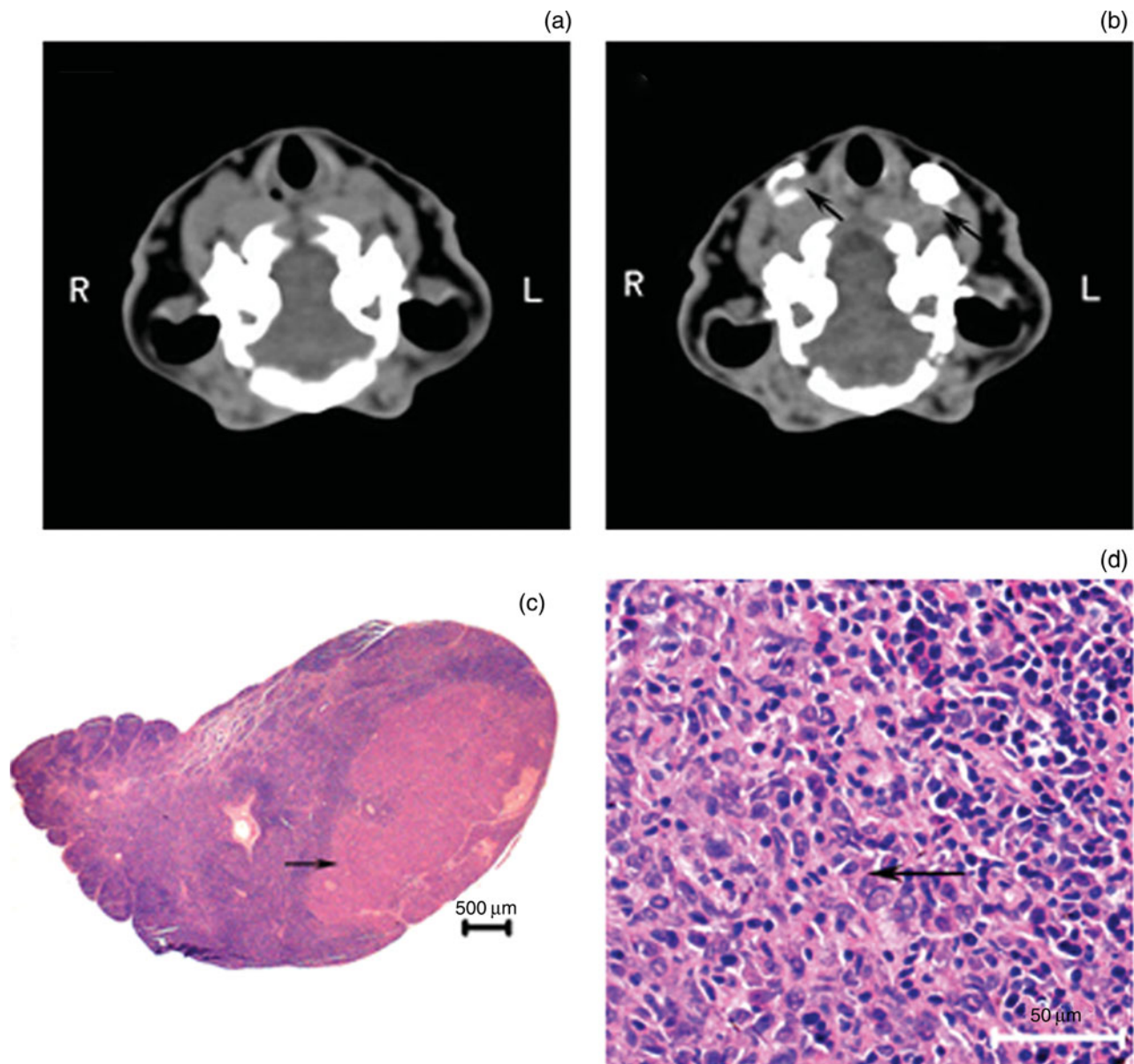


FIG. 1

Investigation results for a rabbit imaged and sacrificed 21 days after carcinoma implantation. (a) Axial computed tomography (CT) scan taken before administration of contrast agent, showing no noticeable lymph node enhancement. (b) Axial CT scan taken after administration of contrast agent, showing lymph node enhancement indicating an ipsilateral (right) filling defect (arrow to left of figure part) and a contralateral (left) rounded lymph node shape (arrow to right of figure part). Histopathological analysis (H&E staining) indicated that the right-sided enhanced lymph node was metastatic (1c ( $\times 25$ ) and 1d ( $\times 200$ ); arrows), while the left-sided enhanced lymph node was non-metastatic. (Note that the CT lymphography image and histopathological specimens do not exactly align, as the section orientation was not identical.) R = right; L = left

After iopamidol injection, indirect CT lymphography revealed rapid, bilateral enhancement of afferent lymphatic vessels and cervical lymph nodes with diameters greater than those of lymphatic vessels. The enhanced cervical lymph nodes were all in the same position, i.e. lateral to the larynx and cricoid cartilage, below the sternothyroid muscle (Figure 1b).

In one animal imaged and sacrificed 28 days after carcinoma implantation, the contralateral lymph node was enhanced together with bilateral afferent lymphatic vessels (Figure 2c and 2d), while the ipsilateral lymph node was not enhanced in any CT lymphography image.

The mean  $\pm$  SD CT attenuation values of enhanced metastatic lymph nodes were  $561.6 \pm 102.5$ ,  $472.2 \pm 98.1$ ,  $342.9 \pm 82.7$ ,  $219.3 \pm 71.3$ ,  $144.3 \pm 52.1$  and  $91.1 \pm 39.0$  Hounsfield Unit (HU) at 1, 3, 5, 10, 15 and 20 minutes after iopamidol injection, respectively. Corresponding values for non-metastatic lymph nodes were  $640.0 \pm 173.5$ ,  $508.4 \pm 144.3$ ,  $342.2 \pm 107.3$ ,  $201.0 \pm 64.1$ ,  $116.5 \pm 37.5$  and  $67.9 \pm 20.5$  HU, respectively. There was a significantly slower 'wash-out' slope ( $p < 0.001$ ) in metastatic lymph nodes compared with non-metastatic lymph nodes, at all six assessment times (i.e. 1, 3, 5, 10, 15 and 20 minutes) after iopamidol injection (Figure 3).

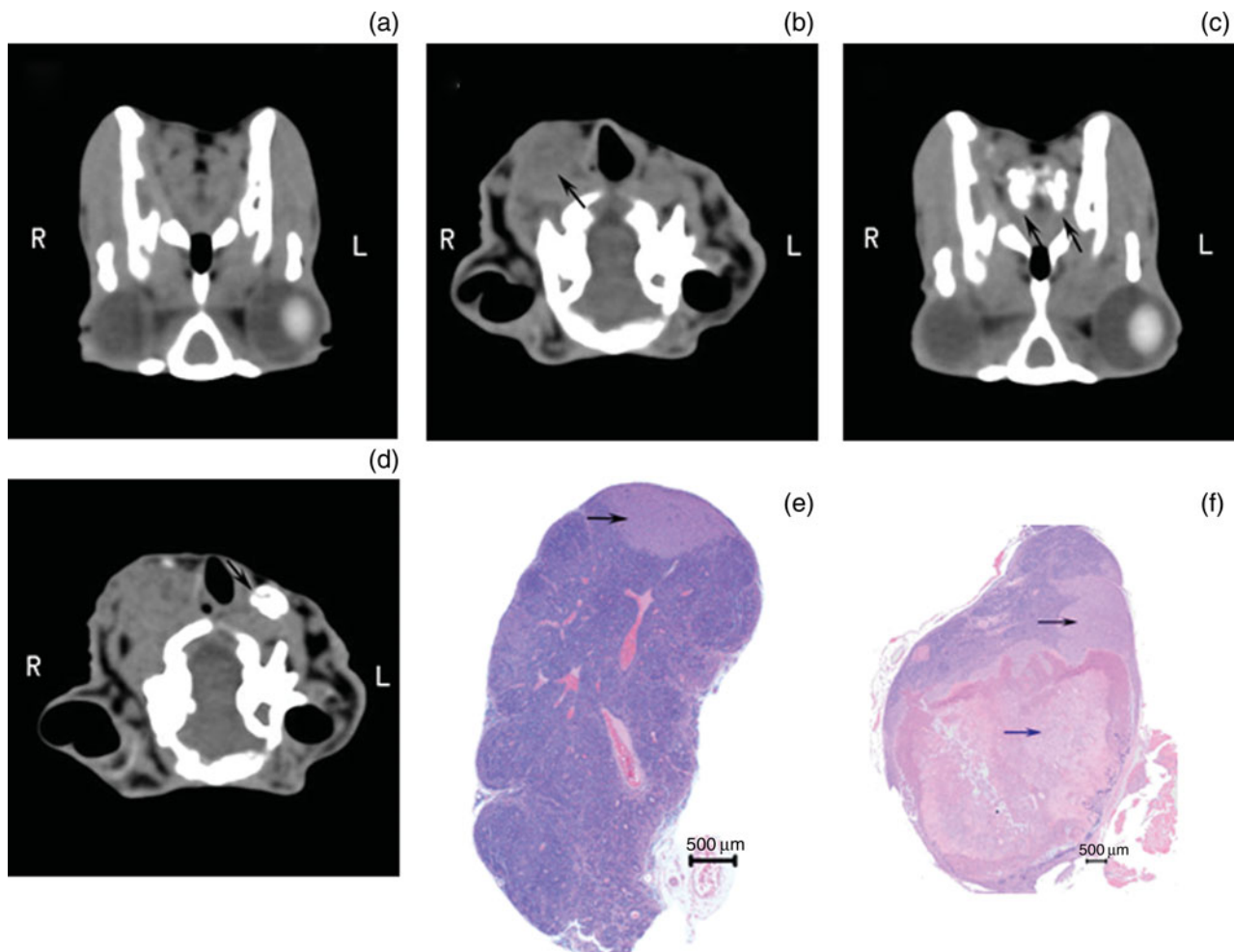


FIG. 2

Investigation results for a rabbit imaged and sacrificed 28 days after carcinoma implantation. Prior to contrast administration, axial computed tomography (CT) showed no clear enhancement of lymphatic vessels (a) or lymph nodes (b); however, an obscured boundary suggested an enlarged right lymph node (b, arrow). After contrast administration, axial CT showed bilateral enhancement of afferent lymphatic vessels (c, arrows) and a filling defect in a contralateral (left) lymph node (d, arrow); the ipsilateral (right) lymph node did not enhance (d). Histopathological analysis (H&E staining) indicated metastasis in the left lymph node (e, arrow;  $\times 25$ ), while the right lymph node was confirmed to be over 80 per cent replaced by metastasis (f, black arrow;  $\times 25$ ) and necrosis (blue arrow). (Note that CT images and histopathological specimens do not exactly align, as the section orientation was not identical. Note also that part (f) is generated using Adobe Photoshop Lightroom (version 2.0) software, as the full image was too large to reproduce.) R = right; L = left

The mean  $\pm$  SD maximum axial diameter was  $7.51 \pm 1.57$  mm for metastatic lymph nodes and  $6.23 \pm 1.71$  mm for non-metastatic lymph nodes.

Enhanced lymph nodes displayed an oval or round shape, or showed local filling defects (Figure 1b). Of the 11 lymph nodes with an oval or round shape, 10 were confirmed to be non-metastatic on histopathological analysis (10/11, 90.9 per cent).

Thirty lymph nodes showed local filling defects; of these, nine were confirmed histopathologically to be non-metastatic (nine of 30, 30 per cent), whereas 21 were metastatic (21/30, 70 per cent).

The mean filling defect diameter and mean intranodal filling defect ratio were both significantly smaller in non-metastatic lymph nodes ( $t = -2.96$ ,  $p = 0.0062$ , and  $z = -2.83$ ,  $p = 0.0047$ , respectively) compared with metastatic nodes (Table I).

In the animal with a non-enhanced ipsilateral lymph node, imaged on day 28 after carcinoma implantation, this same lymph node was subsequently seen, on histopathological examination, to be nearly completely replaced by metastases, with a maximum axial diameter of 13 mm (Figure 2f).

We investigated the use of lymph node filling defect diameter and intranodal filling defect ratio as criteria for the differentiation of metastatic versus non-metastatic lymph nodes. Table II lists different possible diagnostic thresholds for these two parameters. The use of a filling defect diameter of 1.5 mm as a diagnostic criterion for lymph node metastasis had a sensitivity, specificity, accuracy, and positive and negative predictive values of 86.4 per cent (19/22), 78.9 per cent (15/19), 82.9 per cent (34/41), 82.6 per cent (19/23) and 83.3 per cent (15/18), respectively. The use of an intranodal filling defect ratio of 1:5 for the

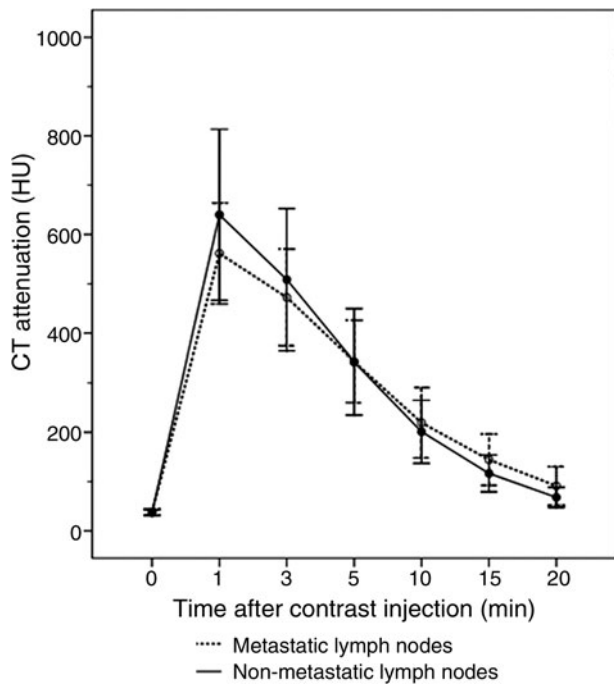


FIG. 3

Mean computed tomography (CT) attenuation of metastatic and non-metastatic lymph nodes over time, before and after contrast injection. Outliers represent standard deviations. Mean CT attenuation was maximal 1 min after contrast injection and decreased over subsequent CT lymphography images; total enhancement time was approximately 20 min. HU = Hounsfield Unit

same diagnostic task had a sensitivity, specificity, accuracy, and positive and negative predictive values of 77.3 per cent (17/22), 78.9 per cent (15/19), 78 per cent (32/41), 81 per cent (17/21) and 75 per cent (15/20), respectively. Calculation of the area under the receiver operating characteristic curve indicated no statistically significant difference between the diagnostic value of filling defect diameter and intranodal filling defect ratio ( $p = 0.8408$ ) (Figure 4).

**Discussion**

Rabbits are commonly utilised as research models for cervical lymph node metastases. Jefferis and Berenbaum identified parotid lymph node metastases following introduction of VX2 carcinoma into the dorsal mucosa of the tongue; however, they did not describe deep cervical lymph node metastases in this study.<sup>21</sup> Seki and Fujimura confirmed histopathologically the

Parameter	Non-met LN*	Met LN†	<i>p</i>
FDD (mm)	1.7 ± 0.7	3.0 ± 1.1	0.0062
IFD ratio	16.5 ± 6.0	27.5 ± 12.1	0.0047

\**n* = 9; †*n* = 21. Non-met LN = non-metastatic lymph nodes; met = metastatic; FDD = filling defect diameter; IFD = intranodal filling defect

TABLE II  
UTILITY OF FILLING DEFECT DIAMETER AND INTRANODAL FILLING DEFECT RATIO AS DIAGNOSTIC CRITERIA FOR NON-METASTATIC VS METASTATIC LYMPH NODES: EFFECT OF DIFFERENT THRESHOLDS

Threshold	Sens	Spec	Acc	PPV	NPV
<i>FDD (mm)</i>					
≥0.5	95.5	52.6	75.6	70.0	90.9
≥1.0	95.5	57.9	78.0	72.4	91.7
≥1.5	86.4	78.9	82.9	82.6	83.3
≥2.0	77.3	78.9	78.0	81.0	75.0
≥2.5	63.6	94.7	78.0	93.3	69.2
≥3.0	40.9	94.7	65.9	90.0	58.1
<i>IFD ratio</i>					
≥1:7	86.4	68.4	78.0	76.0	81.3
≥1:6	81.8	73.7	78.0	78.3	77.8
≥1:5	77.3	78.9	78.0	81.0	75.0
≥1:4	45.5	94.7	68.3	90.9	60.0
≥1:3	27.3	100.0	61.0	100.0	54.3
≥1:2	9.1	100.0	51.2	100.0	48.7

Data represent percentages. Sens = sensitivity; spec = specificity; acc = accuracy; PPV = positive predictive value; NPV = negative predictive value; FDD = filling defect diameter; IFD = intranodal filling defect

presence of deep cervical lymph node metastases 10 days after VX2 carcinoma implantation into the lateral border of the tongue.<sup>22,23</sup> Hamaguchi *et al.* identified deep cervical lymph node metastases following VX7 cell suspension implantation into the left side of the tongue at the lingual margin.<sup>24</sup> In our own previous experiments, CT lymphography enhanced only deep cervical lymph nodes, and ipsilateral or bilateral deep cervical lymph node metastases were confirmed by histopathological analysis. Previous studies utilising indirect CT lymphography have identified no

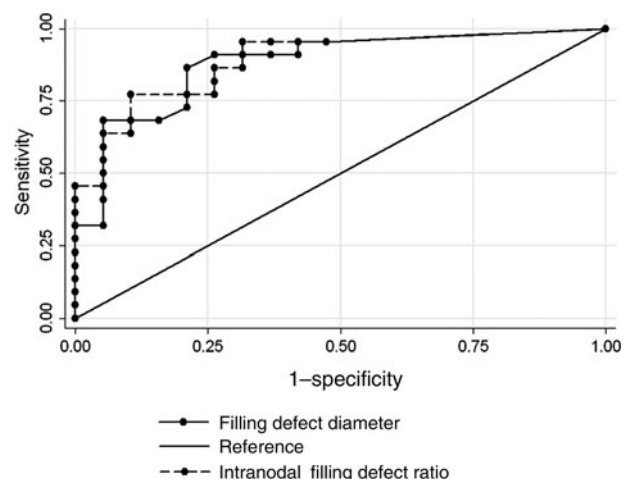


FIG. 4

Receiver operating characteristic curves for filling defect diameter and intranodal filling defect ratio, for the detection of metastatic lymph nodes. Az values, representing the area under the receiver operating characteristic curve, were 0.8804 for filling defect diameter (95 per cent confidence intervals (CIs) = 0.77391, 0.98686) and 0.8900 for intranodal filling defect ratio (95 per cent CIs = 0.79097, 0.98893), as determined from computed tomography lymphography images. There was no statistically significant difference between these Az values ( $p = 0.8408$ ).

enhancement or metastases in the parotid or submandibular lymph nodes of tumour-bearing rabbits.<sup>16,17</sup>

In the present study, we confirmed that the lymph nodes enhanced during indirect CT lymphography were deep cervical lymph nodes, according to their position and size in CT lymphography images and their histopathological results. We found no enhancement or metastases in parotid or submandibular lymph nodes. Moreover, we identified the presence of deep cervical lymph node metastases on days 11 to 28 after VX2 carcinoma implantation; this is consistent with previous findings.<sup>17,18,22,23</sup>

When considering the clinical implications of our results, it is important to note that metastatic lymph node drainage patterns differ between rabbits and humans.

Head and neck cancers (e.g. tongue, supraglottic and hypopharyngeal carcinoma) are often complicated by metastasis to cervical lymph nodes; the rate of occult metastasis to these lymph nodes can be as high as 50 per cent.<sup>25</sup> At present, it is still difficult to differentiate non-enlarged, borderline-sized metastatic lymph nodes without central necrosis or extracapsular spread from those lymph nodes which are enlarged due to reactive or inflammatory processes.<sup>26</sup>

Indirect CT lymphography provides an alternative means of differentiating metastatic from non-metastatic lymph nodes. Although it has sufficient spatial resolution and depiction of local anatomy, CT imaging of intranodal architecture is suboptimal, and can be improved by the use of a contrast agent. When such a contrast agent is used, normal lymph nodes enhance homogeneously while abnormal nodes display clear distortions in the accumulation of contrast agent.<sup>27</sup>

Indirect CT lymphography with iopamidol has recently been used to identify sentinel lymph nodes, and is considered a simple, safe and inexpensive technique for this purpose.<sup>12–15</sup> Iopamidol is a commercially available, water-soluble, iodine-based contrast agent which appears to easily penetrate into the lymphatics through clefts in the terminal lymphangioles of the interstitial space.<sup>28</sup>

In the current study, indirect CT lymphography successfully enhanced cervical lymph nodes. Maximum enhancement occurred 1 minute after iopamidol injection, and the total enhancement time was approximately 20 minutes. Iopamidol may partly drain into the vascular system. However, this volume appears to be negligible; we did not observe any noticeable venous enhancement, nor any potentially negative effects on lymph node investigation. There was a significantly slower wash-out slope in metastatic lymph nodes compared with non-metastatic nodes; this is consistent with previous findings.<sup>10</sup> Fischbein *et al.* reported a reduced transfer of contrast agent to tissue and a decreased volume of extravascular, extracellular space in metastatic lymph node tissue compared with normal or reactive lymph node tissue.<sup>19</sup> We hypothesise that lymphatic drainage is affected by metastatic

carcinoma, with lymph vessel obstruction and tumour cell embolisation delaying the evacuation of contrast agent.

Filling defects are caused by the presence of metastatic tissue, and are considered a very reliable criterion for the diagnosis of lymph node metastases.<sup>29–31</sup> In the present study, enhanced lymph nodes displayed an oval or round shape and/or local filling defects. Seventy per cent of lymph nodes with local filling defects were metastatic, while 90.9 per cent of oval or round lymph nodes were non-metastatic. The mean filling defect diameter and mean intranodal filling defect ratio were significantly smaller in non-metastatic lymph nodes compared with metastatic nodes.

It should be noted that other processes can also lead to filling defects within lymph nodes, such as inflammation, tuberculosis and fatty infiltration.

Stephenson *et al.* used a filling defect diameter of 2 mm, on X-ray lymphography, as a diagnostic criterion for metastatic lymph nodes in cases of seminoma and non-seminomatous germ cell tumours.<sup>29</sup> Voneschenbach *et al.* proposed that the ability of lymphography to demonstrate internal lymph node architecture, and to detect the presence of filling defects 5–7 mm in diameter, made it a useful complement to CT and a useful alternative to surgical lymphadenectomy.<sup>30</sup> Lang recommended the use of a filling defect diameter of 5 mm or an intranodal filling defect ratio of 1:3 as important diagnostic cut-off points for the diagnosis of lymph node metastases of malignant gynaecological tumours, on X-ray lymphography.<sup>31</sup>

We found that the sensitivity, specificity, accuracy, and positive and negative predictive values of the use of a filling defect diameter of 1.5 mm as a diagnostic criterion for lymph node metastases were 86.4 per cent (19/22), 78.9 per cent (15/19), 82.9 per cent (34/41), 82.6 per cent (19/23) and 83.3 per cent (15/18), respectively. The use of an intranodal filling defect ratio of 1:5 had corresponding values of 77.3 per cent (17/22), 78.9 per cent (15/19), 78 per cent (32/41), 81 per cent (17/21) and 75 per cent (15/20), respectively.

In the current study, the diagnostic value of these two tests was not significantly different. The fact that rabbit lymph nodes are substantially smaller than human lymph nodes may be one reason for these findings. Furthermore, CT can provide higher spatial and temporal resolution than X-ray imaging.

Fat replacement or inflammation may lead to a false positive diagnosis of metastatic tumour. False negative diagnoses may occur when tumour completely replaces the node, or when metastases are microscopic and therefore invisible to the eye.<sup>30</sup> It is possible that the false positives in our study may have been caused by an inflammatory reaction. In addition, micrometastases may have been missed during histopathological examination, although this was carefully performed.

In our animal model, we considered results obtained between 14 and 21 days after carcinoma implantation to

indicate early metastatic lymph node staging, and those obtained 28 days after carcinoma implantation to indicate advanced metastatic lymph node staging.<sup>18</sup>

In one rabbit imaged and sacrificed 28 days after carcinoma implantation, the ipsilateral lymph node did not enhance. Histopathological examination indicated that this non-enhanced lymph node was almost completely replaced by metastases, with a maximum axial diameter of 13 mm. This case emphasises the fact that, when CT lymphography results indicate a 'vanished' lymph node, the possibility of lymph node metastasis should be considered. Moreover, our finding could indicate that indirect CT lymphography may not be useful to detect lymph nodes with advanced metastases. However, lymph nodes with advanced metastases may be differentiated using conventional, non-contrast CT scanning. Thus, indirect CT lymphography with iopamidol may have a clinical application in the diagnosis of early lymph node metastases.

- **This study investigated the utility of indirect computed tomography (CT) lymphography with iopamidol in detecting metastatic cervical lymph nodes in a tongue VX2 carcinoma model**
- **All contrast-enhancing lymph nodes displayed either a local filling defect or an oval or round shape; filling defects were seen in most early metastatic nodes**
- **Filling defects and slow evacuation of contrast agent are important features of metastatic lymph nodes visualised by indirect CT lymphography**

The number of animal models used in the current study was relatively limited. However, we viewed this study as a preliminary experiment investigating the feasibility of indirect CT lymphography with iopamidol contrast in differentiating metastatic from non-metastatic lymph nodes. Future research could investigate the optimal dosage of contrast agent, as well as clinical applications in humans.

## Conclusion

These findings suggest that lymph node filling defects and slow evacuation of contrast are important features of indirect CT lymphography used to differentiate metastatic from non-metastatic lymph nodes. Further investigation of this subject area is warranted.

## Acknowledgements

We thank Dr Guixiang Zhang, First People's Hospital of Shanghai, Jiaotong University, for providing the VX2 carcinoma tissue. This study was supported by grants from the Science and Technology Commission of Shanghai Municipality, China (number 09411967500) and the Shanghai Hospital Cooperation Foundation (number SHDC12010119).

## References

- 1 Barrett T, Choyke PL, Kobayashi H. Imaging of the lymphatic system: new horizons. *Contrast Media Mol Imaging* 2006;**1**: 230–45
- 2 Chen J, Cheong JH, Yun MJ, Kim J, Lim JS, Hyung WJ *et al*. Improvement in preoperative staging of gastric adenocarcinoma with positron emission tomography. *Cancer* 2005;**103**:2383–90
- 3 Ng SH, Yen TC, Liao CT, Chang JTC, Chan SC, Ko SF *et al*. F-18-FDG PET and CT/MRI in oral cavity squamous cell carcinoma: a prospective study of 124 patients with histologic correlation. *J Nucl Med* 2005;**46**:1136–43
- 4 Russell M, Anzai Y. Ultrasmall superparamagnetic iron oxide enhanced MR imaging for lymph node metastases. *Radiography* 2007;**13**(Supplement 1):e73–84
- 5 Schoder H, Carlson DL, Kraus DH, Stambuk HE, Gonen M, Erdi YE *et al*. F-18-FDG PET/CT for detecting nodal metastases in patients with oral cancer staged N0 by clinical examination and CT/MRI. *J Nucl Med* 2006;**47**(5):755–62
- 6 Wunderbaldinger P. Problems and prospects of modern lymph node imaging. *Eur J Radiol* 2006;**58**:325–37
- 7 Witte CL, Williams WH, Witte MH. Lymphatic imaging. *Lymphology* 1993;**26**:109–11
- 8 Guermazi A, Brice P, Hennequin C, Sarfati E. Lymphography: an old technique retains its usefulness. *Radiographics* 2003;**23**: 1541–58
- 9 Wolf GL, Rogowska J, Hanna GK, Halpern EF. Percutaneous CT lymphography with Perflubron – imaging efficacy in rabbits and monkeys. *Radiology* 1994;**191**:501–5
- 10 Wisner ER, Katzberg RW, Link DP, Griffey SM, Drake CM, Vessey AR *et al*. Indirect computed tomography lymphography using iodinated nanoparticles to detect cancerous lymph nodes in a cutaneous melanoma model. *Acad Radiol* 1996;**3**: 40–8
- 11 Jiang DY, Gazelle GS, Wolf GL. A model of focal cancer in rabbit lymph nodes. *Acad Radiol* 1996;**3**:159–62
- 12 Takahashi M, Sasa M, Hirose C, Hisaoka S, Taki M, Hirose T *et al*. Clinical efficacy and problems with CT lymphography in identifying the sentinel node in breast cancer. *World J Surg Oncol* 2008;**6**:57
- 13 Suga K, Shimizu K, Kawakami Y, Tangoku A, Zaki M, Matsunaga N *et al*. Lymphatic drainage from esophagogastric tract: feasibility of endoscopic CT lymphography for direct visualization of pathways. *Radiology* 2005;**237**:952–60
- 14 Ueda K, Suga K, Kaneda Y, Li TS, Ueda K, Hamano K. Preoperative imaging of the lung sentinel lymphatic basin with computed tomographic lymphography: a preliminary study. *Ann Thorac Surg* 2004;**77**:1033–8
- 15 Suga K, Karino Y, Fujita T, Okada M, Kawakami Y, Ueda K *et al*. Cutaneous drainage lymphatic map with interstitial multi-detector-row computed tomographic lymphography using iopamidol: preliminary results. *Lymphology* 2007;**40**:63–73
- 16 Wu H, Xu X, Ying H, Hoffman MR, Shen N, Sha Y *et al*. Preliminary study of indirect CT lymphography-guided sentinel lymph node biopsy in a tongue VX2 carcinoma model. *Int J Oral Maxillofac Surg* 2009;**38**:1268–72
- 17 Wu H, Ying H, Xi X, Shen N, Shu Y, Hoffman MR *et al*. Localization of the sentinel lymph node in tongue VX2 carcinoma via indirect CT lymphography combined with methylene blue dye injection. *Acta Otolaryngol (Stockh)* **130**(4):503–10
- 18 Ying H, Wu H, Zhou L. Establishment of the deep cervical lymph node metastasis model of tongue VX2 carcinoma and observation of its metastatic features. *Chinese Journal of Otorhinolaryngology Head and Neck Surgery* 2008;**43**:778–81
- 19 Fischbein NJ, Noworolski SM, Henry RG, Kaplan MJ, Dillon WP, Nelson SJ. Assessment of metastatic cervical adenopathy using dynamic contrast-enhanced MR imaging. *Am J Neuroradiol* 2003;**24**:301–11
- 20 Herbom CU, Lauenstein TC, Vogt FM, Lauffer RB, Debatin JF, Ruehm SG. Interstitial MR lymphography with MS-325: characterization of normal and tumor-invaded lymph nodes in a rabbit model. *Am J Roentgenol* 2002;**179**:1567–72
- 21 Jefferis AF, Berenbaum MC. The rabbit Vx2 tumor as a model for carcinomas of the tongue and larynx. *Acta Otolaryngol (Stockh)* 1989;**108**:152–60
- 22 Seki S, Fujimura A. Three dimensional changes in lymphatic architecture around VX2 tongue cancer – dynamic changes after administration of antiangiogenic agent. *Lymphology* 2003;**36**:199–208

- 23 Seki S, Fujimura A. Three-dimensional changes in lymphatic architecture around VX2 tongue cancer – dynamics of growth of cancer. *Lymphology* 2003;**36**:128–39
- 24 Hamaguchi S, Tohnai I, Ito A, Mitsudo K, Shigetomi T, Ito M *et al.* Selective hyperthermia using magnetoliposomes to target cervical lymph node metastasis in a rabbit tongue tumor model. *Cancer Sci* 2003;**94**:834–9
- 25 Gourin CG, Conger BT, Porubsky ES, Sheils WC, Bilodeau PA, Coleman TA. The effect of occult nodal metastases on survival and regional control in patients with head and neck squamous cell carcinoma. *Laryngoscope* 2008;**118**:1191–4
- 26 Mack MG, Rieger J, Baghi M, Bisdas S, Vogl TJ. Cervical lymph nodes. *Eur J Radiol* 2008;**66**:493–500
- 27 Wolf GL, Gazelle GS, McIntire G, Bacon E, Toner J, Cooper E. Percutaneous computed tomographic lymphography of normal, inflamed, and cancerous nodes in the rabbit. *Invest Radiol* 1994;**29**(Supplement 2):S30–2
- 28 Tangoku A, Seike J, Nakano K, Nagao T, Honda J, Yoshida T *et al.* Current status of sentinel lymph node navigation surgery in breast and gastrointestinal tract. *J Med Invest* 2007;**54**:1–18
- 29 Stephenson NJ, Sandeman TF, McKenzie AF. Has lymphography a role in early stage testicular germ cell tumours? *Australas Radiol* 1995;**39**:54–7
- 30 Voneschenbach AC, Jing BS, Wallace S. Lymphangiography in genitourinary cancer. *Urol Clin North Am* 1985;**12**:715–23
- 31 Lang JH. Lymphangiography in ovarian cancer [in Chinese]. *Zhonghua Fu Chan Ke Za Zhi* 1989;**24**:29–31, 58

Address for correspondence:

Dr Haitao Wu,  
83 FenYang Road, Shanghai 200031,  
PR China

Fax: +086 21 64377151

E-mail: Haitaowu1103@hotmail.com

---

Dr H Wu takes responsibility for the integrity of the content  
of the paper

Competing interests: None declared

---